



HAL
open science

Draft genome sequence of *Promicromonospora panici* sp. nov., a novel ionizing-radiation-resistant actinobacterium isolated from roots of the desert plant *Panicum turgidum*

Sihem Guesmi, Imen Nouioui, Petar Pujic, Audrey Dubost, Afef Najjari, Kais Ghedira, José M Igual, Ameer Cherif, Hans-Peter Klenk, Haïtham Sghaier, et al.

► **To cite this version:**

Sihem Guesmi, Imen Nouioui, Petar Pujic, Audrey Dubost, Afef Najjari, et al.. Draft genome sequence of *Promicromonospora panici* sp. nov., a novel ionizing-radiation-resistant actinobacterium isolated from roots of the desert plant *Panicum turgidum*. *Extremophiles*, 2021, 25 (1), pp.25-38. <10.1007/s00792-020-01207-8>. <hal-03378213>

HAL Id: hal-03378213

<https://hal.science/hal-03378213v1>

Submitted on 14 Oct 2021

HAL is a multi-disciplinary open access archive for the deposit and dissemination of scientific research documents, whether they are published or not. The documents may come from teaching and research institutions in France or abroad, or from public or private research centers.

L'archive ouverte pluridisciplinaire **HAL**, est destinée au dépôt et à la diffusion de documents scientifiques de niveau recherche, publiés ou non, émanant des établissements d'enseignement et de recherche français ou étrangers, des laboratoires publics ou privés.



HAL Authorization

**Draft genome sequence of *Promicromonospora panici* sp.
nov., a novel ionizing-radiation-resistant
actinobacterium isolated from roots of the desert plant
*Panicum turgidum***

Sihem Guesmi, Imen Nouioui, Petar Pujic, Audrey Dubost, Afef Najjari, Kais Ghedira, José Igual, Ameer Cherif, Hans-Peter Klenk, Haïtham Sghaier, et al.

► **To cite this version:**

Sihem Guesmi, Imen Nouioui, Petar Pujic, Audrey Dubost, Afef Najjari, et al.. Draft genome sequence of *Promicromonospora panici* sp. nov., a novel ionizing-radiation-resistant actinobacterium isolated from roots of the desert plant *Panicum turgidum*. *Extremophiles*, Springer Verlag, 2021, 25 (1), pp.25-38. 10.1007/s00792-020-01207-8 . hal-03378213

HAL Id: hal-03378213

<https://hal.archives-ouvertes.fr/hal-03378213>

Submitted on 14 Oct 2021

HAL is a multi-disciplinary open access archive for the deposit and dissemination of scientific research documents, whether they are published or not. The documents may come from teaching and research institutions in France or abroad, or from public or private research centers.

L'archive ouverte pluridisciplinaire **HAL**, est destinée au dépôt et à la diffusion de documents scientifiques de niveau recherche, publiés ou non, émanant des établissements d'enseignement et de recherche français ou étrangers, des laboratoires publics ou privés.

Metadata of the article that will be visualized in OnlineFirst

ArticleTitle	Draft genome sequence of <i>Promicromonospora panici</i> sp. nov., a novel ionizing-radiation-resistant actinobacterium isolated from roots of the desert plant <i>Panicum turgidum</i>	
Article Sub-Title		
Article CopyRight	Springer Japan KK, part of Springer Nature (This will be the copyright line in the final PDF)	
Journal Name	Extremophiles	
Corresponding Author	Family Name	Normand
	Particle	
	Given Name	Philippe
	Suffix	
	Division	
	Organization	Université de Lyon, Université Lyon 1
	Address	Lyon, France
	Division	
	Organization	CNRS, UMR 5557, Écologie Microbienne, UMR1418, INRA
	Address	69622, Villeurbanne Cedex, France
	Phone	
	Fax	
	Email	philippe.normand@univ-lyon1.fr
	URL	
	ORCID	
Author	Family Name	Guesmi
	Particle	
	Given Name	Sihem
	Suffix	
	Division	
	Organization	National Agronomy Institute of Tunisia
	Address	Avenue Charles Nicolle, 1082, Tunis, Mahrajène, Tunisia
	Division	Laboratory “Energy and Matter for Development of Nuclear Sciences” (LR16CNSTN02), National Center for Nuclear Sciences and Technology
	Organization	Sidi Thabet Technopark
	Address	2020, Sidi Thabet, Tunisia
	Phone	
	Fax	
	Email	
	URL	
	ORCID	
Author	Family Name	Nouioui
	Particle	
	Given Name	Imen
	Suffix	

Division School of Natural and Environmental Sciences
Organization Newcastle University
Address Ridley Building 2, Newcastle upon Tyne, NE1 7RU, UK
Division
Organization Leibniz Institute DSMZ-German Collection of Microorganisms and Cell Cultures
Address Braunschweig, Germany
Phone
Fax
Email
URL
ORCID

Author Family Name **Pujic**
Particle
Given Name **Petar**
Suffix
Division
Organization Université de Lyon, Université Lyon 1
Address Lyon, France
Division
Organization CNRS, UMR 5557, Écologie Microbienne, UMR1418, INRA
Address 69622, Villeurbanne Cedex, France
Phone
Fax
Email
URL
ORCID

Author Family Name **Dubost**
Particle
Given Name **Audrey**
Suffix
Division
Organization Université de Lyon, Université Lyon 1
Address Lyon, France
Division
Organization CNRS, UMR 5557, Écologie Microbienne, UMR1418, INRA
Address 69622, Villeurbanne Cedex, France
Phone
Fax
Email
URL
ORCID

Author Family Name **Najjari**
Particle
Given Name **Afef**

Suffix
Division
Organization Université de Tunis el Manar, Faculté des Sciences de Tunis, LR03ES03
Microorganismes et Biomolécules Actives
Address 2092, Tunis, Tunisia
Phone
Fax
Email
URL
ORCID

Author Family Name **Ghedira**
Particle
Given Name **Kais**
Suffix
Division Laboratory of Bioinformatics, Biomathematics and Biostatistics-LR16IPT09
Organization Institut Pasteur de Tunis, Université de Tunis El Manar
Address 1002, Tunis, Tunisia
Phone
Fax
Email
URL
ORCID

Author Family Name **Igual**
Particle
Given Name **José M.**
Suffix
Division
Organization Instituto de Recursos Naturales y Agrobiología de Salamanca, Consejo Superior de Investigaciones Científicas (IRNASA-CSIC)
Address c/Cordel de Merinas 40-52, 37008, Salamanca, Spain
Phone
Fax
Email
URL
ORCID

Author Family Name **Cherif**
Particle
Given Name **Ameur**
Suffix
Division
Organization University Manouba, ISBST, BVBGR-LR11ES31,
Address Biotechpole Sidi Thabet, 2020, Ariana, Tunisia
Phone
Fax
Email
URL

 ORCID

Author	Family Name	Klenk
	Particle	
	Given Name	Hans-peter
	Suffix	
	Division	School of Natural and Environmental Sciences
	Organization	Newcastle University
	Address	Ridley Building 2, Newcastle upon Tyne, NE1 7RU, UK
	Phone	
	Fax	
	Email	
	URL	
	ORCID	

Author	Family Name	Sghaier
	Particle	
	Given Name	Haïtham
	Suffix	
	Division	Laboratory “Energy and Matter for Development of Nuclear Sciences” (LR16CNSTN02), National Center for Nuclear Sciences and Technology
	Organization	Sidi Thabet Technopark
	Address	2020, Sidi Thabet, Tunisia
	Division	
	Organization	University Manouba, ISBST, BVBGR-LR11ES31,
	Address	Biotechpole Sidi Thabet, 2020, Ariana, Tunisia
	Phone	
	Fax	
	Email	
	URL	
	ORCID	

Schedule	Received	24 May 2019
	Revised	
	Accepted	7 October 2020

Abstract

A novel strain of the genus *Promicromonospora*, designated PT9^T, was recovered from irradiated roots of the xerophyte *Panicum turgidum* collected from the Ksar Ghilane oasis in southern Tunisia. Strain PT9^T is aerobic, non-spore-forming, Gram- positive actinomycete that produces branched hyphae and forms white to yellowish-white colonies. Chemotaxonomic features, including fatty acids, whole cell sugars and polar lipid profiles, support the assignment of PT9^T to the genus *Promicromonospora*. The genomic relatedness indexes based on DNA-DNA hybridization and average nucleotide identity values revealed a significant genomic divergence between strain PT9^T and all sequenced type strains of the taxon. Phylogenomic analysis showed that isolate PT9^T was most closely related to *Promicromonospora soli* CGMCC 4.7398^T. Phenotypic and phylogenomic analyses suggest that isolate PT9^T represents a novel species of the genus *Promicromonospora*, for which the name *Promicromonospora panici* sp. nov. is proposed. The type strain is PT9^T (LMG 31103^T = DSM 108613^T). The isolate PT9^T is an ionizing-radiation-resistant actinobacterium (D_{10} value = 2.6 kGy), with resistance to desiccation and hydrogen peroxide. The complete genome sequence of PT9^T consists of 6,582,650 bps with 71.2% G+C content and 6291 protein-coding sequences. This genome will help to decipher the microbial genetic bases for ionizing-radiation resistance mechanisms including the response to oxidative stress.

Keywords (separated by '-') Ionizing-radiation resistant - Genome sequence - Ksar Ghilane oasis - Polyphasic taxonomy - *Promicromonospora panici* - Oxidative stress

Footnote Information Communicated by A. Oren.
Electronic supplementary material The online version of this article (<https://doi.org/10.1007/s00792-020-01207-8>) contains supplementary material, which is available to authorized users.

2 Draft genome sequence of *Promicromonospora panici* sp. nov., a novel 3 ionizing-radiation-resistant actinobacterium isolated from roots 4 of the desert plant *Panicum turgidum*

5 Sihem Guesmi^{1,2} · Imen Nouioui^{3,4} · Petar Pujic^{5,6} · Audrey Dubost^{5,6} · Afef Najjari⁷ · Kais Ghedira⁸ · José M. Igual⁹ ·
6 Ameer Cherif¹⁰ · Hans-peter Klenk³ · Haïtham Sghaier^{2,10} · Philippe Normand^{5,6}

7 Received: 24 May 2019 / Accepted: 7 October 2020
8

9 Abstract

10 A novel strain of the genus *Promicromonospora*, designated PT9^T, was recovered from irradiated roots of the xerophyte
11 *Panicum turgidum* collected from the Ksar Ghilane oasis in southern Tunisia. Strain PT9^T is aerobic, non-spore-forming,
12 Gram-positive actinomycete that produces branched hyphae and forms white to yellowish-white colonies. Chemotaxonomic
13 features, including fatty acids, whole cell sugars and polar lipid profiles, support the assignment of PT9^T to the genus *Promi-*
14 *cromonospora*. The genomic relatedness indexes based on DNA-DNA hybridization and average nucleotide identity values
15 revealed a significant genomic divergence between strain PT9^T and all sequenced type strains of the taxon. Phylogenomic
16 analysis showed that isolate PT9^T was most closely related to *Promicromonospora soli* CGMCC 4.7398^T. Phenotypic and
17 phylogenomic analyses suggest that isolate PT9^T represents a novel species of the genus *Promicromonospora*, for which
18 the name *Promicromonospora panici* sp. nov. is proposed. The type strain is PT9^T (LMG 31103^T = DSM 108613^T). The
19 isolate PT9^T is an ionizing-radiation-resistant actinobacterium (D_{10} value = 2.6 kGy), with resistance to desiccation and
20 hydrogen peroxide. The complete genome sequence of PT9^T consists of 6,582,650 bps with 71.2% G+C content and 6291
21 protein-coding sequences. This genome will help to decipher the microbial genetic bases for ionizing-radiation resistance
22 mechanisms including the response to oxidative stress.

23 **Keywords** Ionizing-radiation resistant · Genome sequence · Ksar Ghilane oasis · Polyphasic taxonomy ·
24 *Promicromonospora panici* · Oxidative stress

25 Abbreviations

26	DSBs	Double-strand breaks
27	ROS	Reactive oxygen species
28	ANI	Average nucleotide identity
29	isDDH	In silico DNA-DNA hybridization
30	IR	Ionizing radiation
31	kGy	Kilogray
32	TSA	Tryptic soy agar
33	TSB	Tryptic soy broth
34		

A1 Communicated by A. Oren.

A2 **Electronic supplementary material** The online version of this
A3 article (<https://doi.org/10.1007/s00792-020-01207-8>) contains
A4 supplementary material, which is available to authorized users.

A5 ✉ Philippe Normand
A6 philippe.normand@univ-lyon1.fr

A7 Extended author information available on the last page of the article

Introduction

The genus *Promicromonospora*, belonging to the family *Promicromonosporaceae*, was first proposed by Krasil'nikov et al. (1961). This genus is phylogenetically closely related to the genera *Cellulosimicrobium* and *Oerskovia* (Schumann et al. 2001; Busse et al. 2003). Members of the genus are aerobic and Gram-positive actinomycetes. Their major characteristics are a branched substrate mycelium that fragments into rod-shaped or coccoid elements, iso- and anteiso-branched as the predominant cellular fatty acids, MK-9(H₄) as the major menaquinone and a DNA G+C content of 70–75% (Schumann and Stackebrandt 2012).

Promicromonospora genus contains 18 species that have been isolated from various biotopes, such as air in the medieval Vienna (Busse et al. 2003), medicinal plant *Maytenus austroyunnanensis* in Yunnan Province (Qin et al. 2012), the surface-sterilized root of a pine tree in Australia (Kaewkla et al. 2017), soil in Mount Song (Zheng et al.

2017), etc. However, it is important to note that the number of validly named species is 14 as of August 08, 2020, available at <https://lpsn.dsmz.de/genus/promicromonospora>, including *Promicromonospora soli* (Zheng et al. 2017), *Promicromonospora kermanensis* (Mohammadipanah et al. 2017), *Promicromonospora callitridis* (Kaewkla and Franco 2017), *Promicromonospora alba* (Guo et al. 2016) and *Promicromonospora iranensis* (Mohammadipanah et al. 2014), among the most recently described species.

Promicromonospora strains have industrially and environmentally valuable applications owing to the production of various bioactive molecules (Gabani and Singh 2013; Thomas et al. 2016), such as antibiotics (Izumikawa et al. 2011), xylanase (Kumar et al. (2011), cellulase (Thomas et al. 2016), xylanilyticolides (Jin et al. 2018), etc. Furthermore, *Promicromonospora* genus showed interesting biological properties, such as antimicrobial activity against bacteria and yeast pathogens (Zothanpuia et al. 2018), bioremediation by the removal of cadmium from polluted waste (Hamedi et al. 2015), plant growth-promoting rhizobacterium through the production of gibberellins (Kang et al. 2012, 2014), etc.

Despite the potential applications of *Promicromonospora* species, there have been a limited number of reports that investigated genomic and phenotypic aspects such as multi-resistance to extreme conditions (radiation, desiccation, oxidative stress, etc.) of this genus members. The number of related genomes available at the National Center for Biotechnology Information (NCBI) and the Genomes OnLine Database is limited to 25 as of August 08, 2020.

In this study, we report the phenotypic, phylogenetic and genomic characterization of a novel actinomycete species, *Promicromonospora panici* sp. nov., with insights into its tolerance to ionizing radiation (IR), desiccation and oxidative stress.

Materials and methods

Strain isolation and cultivation

PT9^T was isolated from irradiated roots of *P. turgidum*, which were collected in May 2015 from the oasis Ksar Ghilane (Tunisia, coordinates N 32°59.557', E 9°36.941', 221.9 m above sea level) at the gates of the Sahara Desert. One-gram root sample aliquots were exposed to levels of IR at a dose of 10 kilogray (kGy) with a mean rate dose of 25.6 kGy/h at room temperature using a cobalt-60 gamma irradiator at the National Center for Nuclear Sciences and Technology (CNSTN), Tunisia. After gamma irradiation, the 1 g root samples were mixed with 9 mL of 0.9% NaCl solution (w/v) and shaken on a rotary shaker at 250 rpm, 30 °C for 1 h (h). Then, 100 µL sample of the suspension

was serially diluted (10^{-5} – 10^{-9}) and spread onto tryptic soy agar (TSA) medium (contains 15 g/L of tryptone, 5 g/L of soy peptone, 5 g/L of sodium chloride and 15 g/L of bacteriological agar, at pH 7). After 7 days of aerobic incubation at 30 °C, colonies were transferred and purified on liquid medium using tryptic soy broth (TSB) and maintained as 20% (v/v) glycerol suspensions at – 20 and – 80 °C (Rainey et al. 2005).

For routine work, PT9^T was cultured aerobically on solid TSA medium and liquid TSB medium for 3 days at 30 °C. Isolate PT9^T was deposited in the BCCM collection (Belgian Coordinated Collections of Microorganisms) and the DSMZ collection (Deutsche Sammlung von Mikroorganismen und Zellkulturen GmbH) under the deposit numbers LMG 31,103 and DSM 108,613, respectively.

Morphological and phenotypic characteristics

Colony morphology of isolate PT9^T was observed by using cells grown on TSA at 30 °C for 2 days. Gram staining was assessed using the standard Gram stain method and spore motility was carried out by optical light and epifluorescence microscopy (Leica Microsystems, Germany) observation of cells suspended in phosphate buffer (at pH 7). For the observation of morphological characteristics, bacterial cells growing on TSA medium at 30 °C for 72 h, were harvested with 2% glutaraldehyde in saline solution (0.9% of NaCl) and then fixed cells were dried in a graded ethanol series (50, 70, 90 and 100% of ethanol) (Kaewkla and Franco 2019). Observations were done via a scanning electron microscope (JSM 5400.JEOL, Japan).

Growth of isolate was checked on Luria–Bertani (LB) (sodium chloride 10 g/L, tryptone 10 g/L, yeast extract 5 g/L), nutrient agar (meat extract 10 g/L, peptone 10 g/L, sodium chloride 5 g/L, agar 15 g/L at pH 7.3), R2YE medium (is a variation of R2 containing yeast extract) (sucrose 10.3 g/L, K₂SO₄ 0.25 g/L, MgCl₂·6H₂O 10.12 g/L, glucose 10 g/L, casamino acid 0.1 g/L, yeast extract 5 g/L, agar 15 g/L), soya flour mannitol agar (soya flour 2 g/l, mannitol 20 g/L, agar 20 g/L), starch casein agar (starch 10 g/L, casein powder 10 g/L, agar 15 g/L at pH 7.2) and in TSA medium at 30 °C for 72 h. The optimal temperature for growth was tested by checking growth on TSA over a range of 10–60 °C with 5 °C intervals. The pH range for growth was examined over a range pH 4–10 with 1 pH unit intervals in TSB over 3 days of incubation at 30 °C. Tolerance of NaCl was evaluated in TSB supplemented with 0–15.0% (w/v) NaCl (at 2.0% intervals) after incubation at 30 °C for 72 h.

Catalase activity was determined by monitoring generation of bubbles upon the addition of a drop of 3% hydrogen peroxide (H₂O₂) solution (Smibert and Krieg 1994).

151 Oxidase activity was assessed by the oxidation of 0.2%
152 (w/v) oxidase reactive by monitoring the colour change.

153 For chemotaxonomic characterization, cells of PT9^T
154 were maintained on yeast extract—malt extract agar (Inter-
155 national Streptomyces Project medium 2; ISP2) medium
156 which had been shaken at 180 rpm and incubated for
157 7 days at 28 °C. After incubation, the biomass of isolate
158 PT9^T was harvested from ISP2 broth cultures. Then, cells
159 were washed three times with sterile distilled water and
160 freeze-dried. Whole-cell sugars were extracted according
161 to the procedures of Lechevalier and Lechevalier (1970)
162 and identified using thin layer chromatography (TLC) as
163 described by Staneck and Roberts (1974). Whole-organism
164 diaminopimelic acids were identified using the protocols
165 of Schleifer and Kandler (1972). Polar lipids pattern was
166 determined following the modified protocol of Minnikin
167 et al. (1984) by Kroppenstedt and Goodfellow (2006). Cel-
168 lular fatty acids were extracted according to the protocol
169 of Miller (1982) with minor modification from Kuykendall
170 et al. (1988). Fatty acid patterns were determined from
171 the biomass of isolate PT9^T using the Standard Microbial
172 Identification (MIDI) system Version 4.5 and the ACTIN6
173 database (Sasser 1990).

174 Genome sequencing, molecular and phylogenetic 175 analyses

176 Genomic DNA extraction

177 Genomic DNA extraction from isolate PT9^T was per-
178 formed as described previously by Marmur (1961) with a
179 phenol/chloroform extraction step (Li et al. 2007). Cells
180 from 50 mL cultures grown on TSB were collected by
181 centrifugation (Eppendorf France) and the pellets were
182 solubilized in 8 mL of 10 mM Tris–HCl at pH 8, 10 mg/
183 mL of lysozyme and 1 mM of ethylenediaminetetraacetic
184 acid (EDTA). Cells lysis was done on the ice during one
185 hour, then 8 mL of 2% w/vol sodium dodecyl sulfate (SDS)
186 and 2.8 mg/mL of proteinase K were added to the mix and
187 incubated at 55 °C for 5 h. Proteins and cell debris were
188 removed by extraction with 16 mL of phenol, chloroform
189 and isoamyl alcohol 25:24:1 (v/v/v) at pH 8.2. After cen-
190 trifugation, the aqueous phase was transferred into a new
191 tube and genomic DNA was precipitated by adding 1.5 mL
192 of 3 M sodium acetate and two volume of absolute ethanol.
193 The DNA pellet was washed in 70% ethanol, air-dried and
194 solubilized in TE buffer (Tris–EDTA buffer from Invit-
195 rogenTM, 10 mM Tris and 0.1 mM EDTA) at pH 8. The
196 quality of extracted DNA was assessed by measuring the
197 A₂₆₀/A₂₈₀ ratio using a Nanodrop (Implen NP80, Thermo
198 Fisher Scientific, USA) spectrophotometer.

Genome sequencing, assembly and annotation

The genome sequencing of PT9^T was performed on the Illu-
minia MiSeqTM platform (Illumina, USA) by Biofidal society,
Vaulx-en-Velin, France (<https://www.biofidal-lab.com>) using
NextGen High Throughput Sequencing. Thus, a standard
Illumina shotgun library “Nextera XT DNA Library Prep”
was constructed and sequenced using the Illumina MiSeq
technology by synthesis. A paired-end sequencing strategy
was used with an average size of 2 × 300 bp in length gener-
ated and a total number of reads of 25,425,220 bp obtained.
Quality control of raw data was assessed using the FastQC
tool ([https://www.bioinformatics.babraham.ac.uk/projects/
fastqc](https://www.bioinformatics.babraham.ac.uk/projects/fastqc)). The Unicycler software was used for de novo assem-
bly. Genome annotation was performed with the Micro-
Scope platform version 3.10.0 using the integrated micro-
bial genomes non-redundant database, KEGG and COG
databases (Vallenet et al. 2017). Reads were processed and
assembled as described by Castro-Wallace et al. (2017). The
final draft assembly had an average depth coverage of 6.9
Mbp and 59 contigs. In addition, the percentage of G + C
in the complete genome sequence was calculated.

Phylogenetic analysis and genomic comparisons

Analysis of the 16S rDNA gene used the complete sequence
retrieved from the genome using MAGE platform (Vallenet
et al. 2009). This gene was identical to the 16S rDNA gene
sequence originally deposited in GenBank (MG712873)
after the initial single colony isolation and amplification
by polymerase chain reaction using the universal 27F and
1492R primers (Sun et al. 2010). The resulting 16S rDNA
gene sequence was compared with those of all validly named
species using the EzTaxon database EzBioCloud ([https://
www.ezbiocloud.net/identify/](https://www.ezbiocloud.net/identify/)) (Yoon et al. 2017) and the
web tool leBIBI(QBPP) available at <https://umr5558-bibiserv.univ-lyon1.fr/lebibi/lebibi.cgi>
(Flandrois et al. 2015). The phylogenetic tree highlighting the position of PT9^T rela-
tive to the type strains of the other species within the genus
Promicromonospora was constructed using W-IQ-TREE
software accessed at <https://iqtree.cibiv.univie.ac.at/>, (Tri-
finopoulos et al. 2016) based on the Shimodaira–Hasegawa
approximate likelihood ratio (SH-aLRT) (%) (Guindon et al.
2010) and the ultrafast bootstrap (UFboot) (%) (Minh et al.
2013).

These 16S rDNA sequence data have been submitted to
the DDBJ/EMBL/GenBank databases through [https://submit
t.ncbi.nlm.nih.gov/](https://submit.ncbi.nlm.nih.gov/) under accession number MG712873.
Genome based phylogenetic tree was constructed using a
high throughput web server, Type Strain Genome server
(TYG) available in the Genome to Genome Distance Cal-
culator webserver (Meier-Kolthoff and Göker 2019).

199

200

201

202

203

204

205

206

207

208

209

210

211

212

213

214

215

216

217

218

219

220

221

222

223

224

225

226

227

228

229

230

231

232

233

234

235

236

237

238

239

240

241

242

243

244

245

246

AQ7 7

248 Average nucleotide identity (ANI) values between the
249 genome of isolate PT9^T and those of the type strains of
250 *Promicromonospora* species were calculated using best hits
251 and reciprocal best hits between two genomic datasets as
252 described by Yoon et al. (2017) available at (<https://www.ezbiocloud.net/tools/ani>).
253 The top hits of the 16S rDNA-related strains of PT9^T were identified via the in silico
254 calculation of digital DNA-DNA hybridization (dDDH)
255 values between strains determination, using the Genome-
256 to-Genome Distance Calculator (GGDC) web server (<https://ggdc.dsmz.de/distcalc2.php>) (Goris et al. 2007; Meier-
257 Kolthoff et al. 2013).

260 Growth under extreme conditions

261 The resistance of isolate PT9^T to extreme conditions was
262 assessed under IR, desiccation and hydrogen peroxide stress.
263 The tolerance to gamma irradiation was assayed using cul-
264 tures of PT9^T and *Escherichia coli* grown in TSB medium
265 and LB agar, respectively at 30 °C for 3 days. Thus, *E.*
266 *coli* DH5 α was used as an IR-sensitive bacterium (Beblo-
267 Vranesevic et al. 2018) for comparative analyses. Briefly,
268 bacterial cells were collected, washed twice with a 0.9%
269 NaCl solution, homogenized and subsequently resuspended
270 in the same solution of NaCl. Survival rates after exposure
271 to a range of gamma radiation doses (1–5 kGy) were deter-
272 mined using the 3-(4, 5-dimethyl imidazole-2-yl)-2, 5-diphe-
273 nyltetrazolium bromide (MTT) assay (Mosmann 1983). Bac-
274 terial cells were exposed to levels of gamma irradiation at
275 a dose ranging from 1 to 5 kGy using a cobalt-60 gamma
276 irradiator at the National Center for Nuclear Sciences and
277 Technology (CNSTN), Tunisia. A volume of 10 μ L of MTT
278 solution (5 mg/mL) was added to 100 μ L of irradiated cells
279 and kept in the dark for 3 h at 37 °C. Results are represented
280 with the corresponding controls not exposed to gamma irra-
281 diation, normalized to 100% (Morini et al. 2017). After incu-
282 bation, the absorbance in each well was measured, including
283 blanks, at 570 nm using a microtiter plate reader (Shimadzu,
284 UV-1800). The value of D_{10} (kGy), which is the dose nec-
285 essary for a 90% reduction in Colony Forming Units, was
286 also calculated via RadioP1 (www.radiop.org.tn) (Benhamda
287 et al. 2015) based on our experimental survival data.

288 The desiccation tolerance assay was performed in TSB
289 medium according to Mattimore and Battista (1996).
290 Briefly, 200 μ L of cell suspensions were pipetted into ster-
291 ile Petri dishes and dried 28 days in a desiccator at 30 °C.
292 *E. coli* DH5 α was used as a desiccation-sensitive bacterium
293 (Beblo-Vranesevic et al. 2018) for comparative analyses.
294 After 28 days, samples were revived by washing the cells
295 off the plate with 200 μ L of saline solution (0.9% NaCl)
296 to rehydrate the cells. Cell viability was examined using
297 MTT assay, then 100 μ L of cell suspensions was transferred
298 to a 96-well microplate and a volume of 10 μ L of MTT

299 solution (5 mg/mL) was added. The microplate was incu-
300 bated at room temperature in the dark for 3 h at 37 °C. After
301 incubation, the absorbance of each well, including blank
302 (without cells) which was normalized to 100%, was meas-
303 ured at 570 nm using a microtiter plate reader (Shimadzu,
304 UV-1800). The measured absorbance at OD 570 nm is pro-
305 portional to the number of viable cells. The survival rate
306 represents the absorbance at 570 nm after drying with a
307 reference before drying. The package lethal (<https://github.com/hofnerb/lethal>)
308 was used also to estimate the survival
309 of PT9^T following exposure to desiccation.

310 Growth of isolate PT9^T with various concentrations of
311 H₂O₂ (v/v) was also performed as described by Gholami
312 et al. (2015). *E. coli* DH5 α was used as a proteome-oxida-
313 tion-sensitive bacterium (Krisko et al. 2010) for comparative
314 analyses. Fifty μ L of bacterial suspensions were added to
315 100 μ L of TSB supplemented with 0–5% (v/v) of H₂O₂ using
316 96-well microplates. Plates were kept in the dark at 30 °C
317 for 48 h with agitation at 120 rpm. The optical density was
318 determined at 630 nm using a microplate reader TECAN
319 (Infinite[®] 200 PRO, Germany).

Prediction of secondary metabolite clusters and genes related to oxidative stress response

322 Clusters for secondary metabolites of isolate PT9^T were pre-
323 dicted using the antiSMASH (<https://antismash.secondarymetabolites.org#!/start>)
324 version 4.0.2 software (Weber et al. 2015). Besides, in silico analyses of the genome PT9^T were
325 done and genes implicated in scavenging of reactive oxygen
326 species (ROS) were determined.
327

Nucleotide sequence accession number

328
329 The whole-genome shotgun sequence of isolate PT9^T
330 was submitted to GenBank/ENA under BioProject acces-
331 sion number PRJEB29453 (ERP111755), BioSample
332 number SAMEA5056529 and SRA accession number
333 ERS2867704. Contig sequences of the de novo assembly
334 were deposited at EMBL under the accession numbers
335 UWYY01000000–UWYY01000056.

Results and discussion

Cultural and phenotypic characteristics

337
338 PT9^T was isolated from the irradiated roots of *Panicum tur-*
339 *gidum*, which were collected from the oasis of Ksar Ghilane
340 in the south of Tunisia. The isolate is an aerobic, Gram-
341 positive, non-motile and non-spore-forming actinomycete.
342 Colonies are white-pigmented on TSA medium (Fig. S1),
343 like *P. xylanilytica*, which was isolated from the medicinal

344 plant *Maytenus austroyunnanensis* (Qin et al. 2012). Cells
 345 of PT9^T developed a branched substrate mycelium with a
 346 wrinkled and shining surface, the septate hyphae of which
 347 broke, at a later stage, into fragments of various sizes and
 348 rod-shaped elements (Fig. 1). This feature is shared by all
 349 members of the genus *Promicromonospora* (Krasil'nikov
 350 et al. 1961; Schumann and Stackebrandt 2012).

351 This actinobacterial isolate had an optimal growth on
 352 nutrient agar, R2YE (medium specific for *Streptomyces*
 353 genus), soya flour mannitol agar and TSA media after incu-
 354 bation at 30 °C for 72 h. It grew moderately well on LB agar
 355 and starch casein agar media. Growth of isolate PT9^T was
 356 observed at 28–37 °C (optimum at 30 °C) and pH 6.0–9.0,
 357 like *P. xylanilytica* YIM 61515^T (Qin et al. 2012). No
 358 growth was observed in the presence of 2% NaCl. Catalase
 359 and oxidase activities of PT9^T were positive, similar to *P.*
 360 *xylanilytica* YIM 61515^T (Qin et al. 2012). *Promicromonos-*
 361 *pora sukumoe* was shown to have a very high endo-cellulase
 362 activity (Ventorino et al. 2015).

363 Chemotaxonomic characteristics

364 Chemotaxonomic features of isolate PT9^T matched those
 365 described for members of the genus *Promicromonospora*.
 366 Whole-organism hydrolysates of isolate PT9^T contained DL-
 367 2,6-Diaminopimelic acid (DL-DAP) and galactose, glucose
 368 and ribose as whole cell sugars. These traits are the same as
 369 the close phylogenetic neighbor, *P. soli* CGMCC 4.7398^T
 370 (Zheng et al. 2017).

371 Polar lipid profiles of PT9^T consisted of diphosphatidyl-
 372 glycerol (DPG), phosphatidylglycerol (PG), phosphatidylin-
 373 ositol (PI) and unidentified lipid (L), phospholipid (PL),
 374 phosphoglycolipid (PGL) and glycolipids (GL₁₋₃). These
 375 features are coherent with those *P. soli* CGMCC 4.7398^T
 376 (Zheng et al. 2017) (Fig. S2). The major fatty acids (>25%)

of PT9^T are *anteiso*-C_{15:0} (56.4%) and *iso*-C_{15:0} (26.9%)
 (Table S1), which are similar to those of *P. soli* CGMCC
 4.7398^T (Zheng et al. 2017).

The chemotaxonomic features of isolate PT9^T are in line
 with the genus *Promicromonospora* but are not enough to
 distinguish isolate PT9^T from its close neighbor. For this
 reason, phylogenetic analyses based on genomic compari-
 sons were necessary to determine the taxonomic affiliation
 of isolate PT9^T.

386 Phylogeny and genomic comparisons

Blast of the complete 16S rDNA gene sequence (1508 bp) of
 isolate PT9^T showed similarity values of 99.3% and 99.0%
 with *P. xylanilytica* YIM 61515^T, *Promicromonospora aereo-*
 389 *lata* DSM 15943^T and *P. iranensis* DSM 45554^T, respec-
 390 tively. However, it decreased to 98.9%, 98.8%, and 98.7%
 391 with *Promicromonospora vindobonensis* DSM 24547^T,
 392 *Promicromonospora thailandica* DSM 26652^T and *P. alba*
 393 DSM 100490^T and *P. callitridis* DSM 103339^T (Table 1),
 394 respectively.

Comparison of the sequences of isolate PT9^T and type
 strains belonging to genus *Promicromonospora* revealed
 identity differences that are marginally within the cut-off
 value of > 1.3% (Stackebrandt and Ebers 2006).

The results of the 16S rDNA gene sequence similarity
 are not in line with the phylogenetic position of strain PT9^T
 in the 16S rDNA gene based tree (Fig. S3). Strain PT9^T
 occupied a poorly supported distinct branch loosely associ-
 ated to a subclade housing several *Promicromonospora* spp.
 including the ones cited above and next to the type strain of
P. soli. Thus, further information is required to determine the
 reliable phylogenetic position of isolate PT9^T.

In the genome based phylogenetic tree (Fig. 2), strain
 PT9^T was found to form a well-supported subclade closely
 related to the type strain of *P. soli* which was associated
 to the branch of *Promicromonospora umidemergens* DSM
 22081^T.

16S rDNA gene sequence similarities between PT9^T and
 closely related type strains indicated the need to confirm
 the genomic distinctness of the type strain as representing a
 novel species by genomic relatedness indices. These analy-
 ses are necessary to further differentiate PT9^T from other
 species affiliated to the *Promicromonospora* genus.

Therefore, pairwise comparisons between isolate
 PT9^T and the available reference genomes were deter-
 mined based on the proposed thresholds for recognition
 of genomic species, ANI and isDDH values. ANI values
 between *P. panici* PT9^T and closely related species ranged
 from 84.6 with *P. sukumoe* DSM 44121^T to 86.95% with
P. soli CGMCC 4.7398^T, which were below the cut-off
 level (95–96%) for species delineation (Goris et al. 2007;
 Richter and Rossello-Mora 2009). Indeed, strain PT9^T

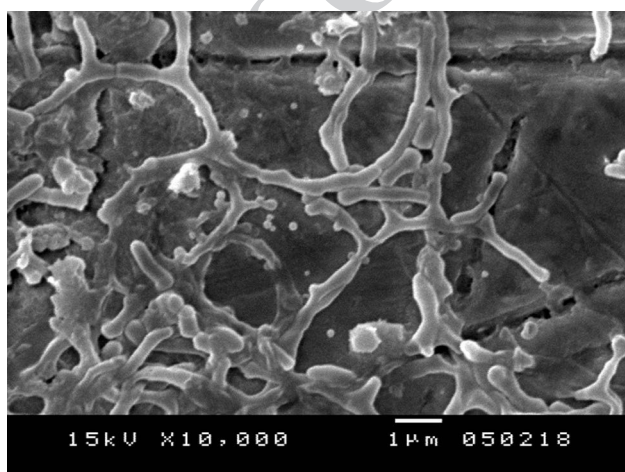


Fig. 1 XXX

Table 1 Identities of the strain PT9^T 16S rDNA gene to those of *Promicromonospora* type strains using EZbiocloud

Rank	Name	Strain	Accession	16S rDNA pairwise similarity(%)
1	<i>Promicromonospora xylanilytica</i>	YIM 61515 ^T	FJ214352	99.3
2	<i>Promicromonospora aerolata</i>	DSM 15943 ^T	AJ487303	99.3
3	<i>Promicromonospora iranensis</i>	DSM 45554 ^T	JN038073	99.0
4	<i>Promicromonospora vindobonensis</i>	DSM 24547 ^T	AJ487302	98.9
5	<i>Promicromonospora thailandica</i>	DSM 26652 ^T	AB560974	98.8
6	<i>Promicromonospora alba</i>	DSM 100490 ^T	KP784765	98.7
7	<i>Promicromonospora callitridis</i>	DSM 103339 ^T	GU434237	98.7
8	<i>Promicromonospora kroppenstedtii</i>	DSM 19349 ^T	KI911710	98.7
9	<i>Promicromonospora endophytica</i>	JCM 19560 ^T	GU434253	98.7
10	<i>Promicromonospora soli</i>	CGMCC 4.7398 ^T	KY352348	98.6
11	<i>Promicromonospora sukumoe</i>	DSM 44121 ^T	AB023375	98.6
12	<i>Promicromonospora citrea</i>	DSM 43110 ^T	X83808	98.5
13	<i>Promicromonospora kermanensis</i>	DSM 45485 ^T	KJ780745	98.5
14	<i>Promicromonospora umidemergens</i>	DSM 22081 ^T	FN293378	98.3

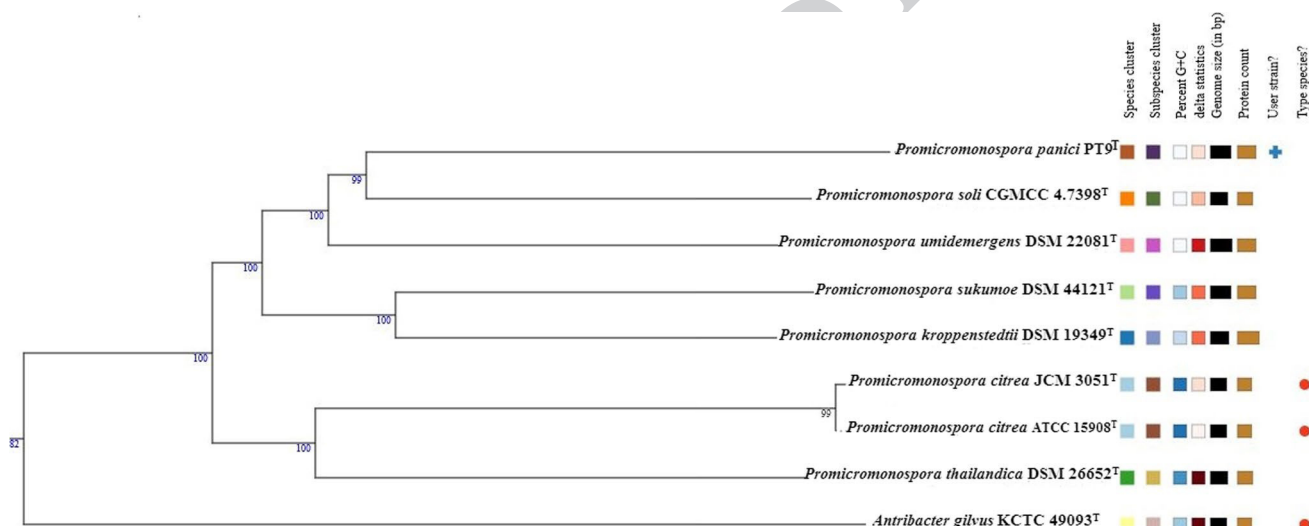


Fig. 2 XXX

428 displayed isDDH value of 32.8% with its closest neighbor
 429 *P. soli* CGMCC 4.7398^T and 31.3% with *Promicromono-*
 430 *spora kroppenstedtii* DSM 19349^T. DNA-DNA related-
 431 ness of 28.8% for isolate PT9^T against *P. sukumoe* DSM
 432 44121^T. These values are well below the 70% cut-off value
 433 recommended for the circumscription of bacterial genomic
 434 species (Wayne et al. 1987; Chun et al. 2018). Thus, isDDH
 435 and ANI values indicated that PT9^T represents a novel spe-
 436 cies within the genus *Promicromonospora*.

437 Based on the morphological, phenotypic and
 438 genetic characteristics, it is evident that isolate PT9^T
 439 should be assigned to a novel species in the
 genus

Promicromonospora, for which the name *Promicromono-*
spora panici sp. nov. is proposed.

Growth under extreme conditions

The survival rate of PT9^T after exposure to IR was assessed.
 PT9^T showed a marked survival profile following treatment
 with increasing doses of gamma radiation (1–5 kGy), when
 compared to *E. coli* DH5 α (Fig. 3).

As shown in Fig. 3, there is a significant difference
 between survival profiles of PT9^T and the IR-sensitive strain
 DH5 α . Indeed, the D₁₀ value of PT9^T was around 2.6 kGy

440
441

442

443
444
445
446

447
448
449

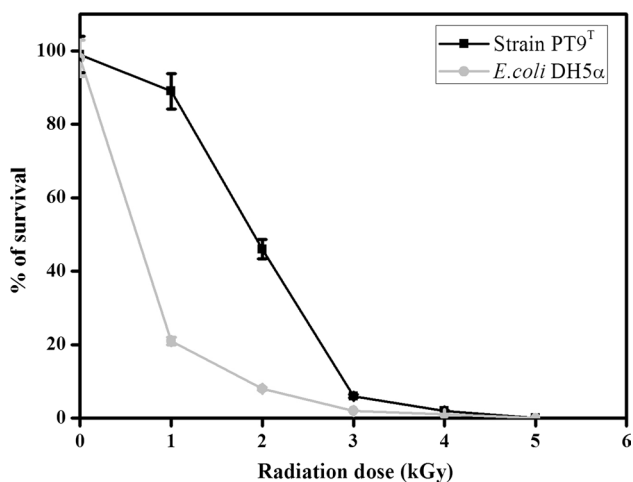


Fig. 3 XXX

(Fig. S4). To be considered an IR-resistant prokaryote, a bacterium should have a D_{10} value greater than 1 kGy (Sghaier et al. 2008). Accordingly, PT9^T (D_{10} = 2.6 kGy) was described as an IR-resistant actinobacterium. Furthermore, the desiccation of isolate PT9^T for 28 days resulted in an overall loss of culturable cells (CFU/mL) of approximately 32% (Fig. S5). Also, the survival rate for this Saharan actinobacterium after 28 days of desiccation was 68% (Fig. S6). Thus, it is legitimate to conclude that PT9^T is also tolerant to desiccation.

The evaluation of resistance to H_2O_2 of PT10 was also assessed at various concentrations from 1 to 5% (v/v) (Fig. 4).

As shown in Fig. 4, PT9^T is tolerant to H_2O_2 at concentrations ranging from 1 to 3% (v/v), when compared to *E. coli* DH5α. However, the growth of PT9^T was almost completely inhibited at a concentration of 5% (v/v) of H_2O_2 .

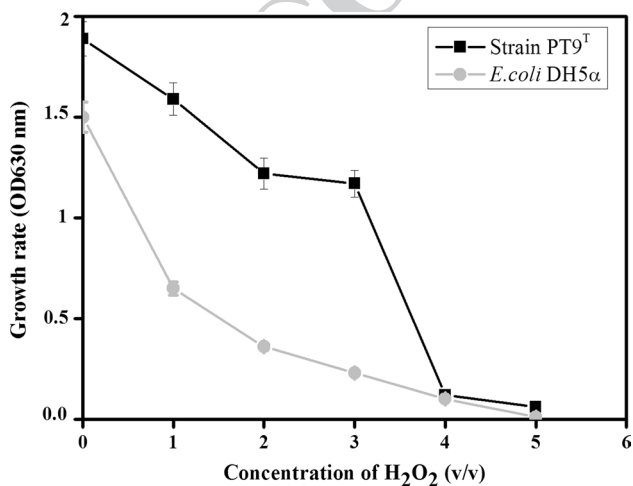


Fig. 4 XXX

Table 2 Genome features of *P. panici* PT9^T

Features	Chromosome
Genome size (bps)	6,582,650
Contig numbers	39
G+C content (%)	71.2
Number of Scaffolds	59
Number of Contigs	59
Average CDS length (bp)	984.18
Protein coding density (%)	91.9
Number of genomic objects	6368
Protein coding genes CDSs	6291
rRNA genes	3
tRNA genes	51

This is the first report that examined the growth under extreme conditions of a strain belonging to genus *Promicromonospora*. Isolate PT9^T is resistant to gamma radiation, desiccation and oxidative stress (H_2O_2). The convergence and the similarity among desiccation and gamma radiation stress response pathways in *Deinococcus radiodurans* were explained by the common production of ROS, which induces oxidative damage to cells (Slade et al. 2011; Lim et al. 2019). Thus, IR-resistant prokaryotes can also be desiccation tolerant (Slade et al. 2011). However, it is necessary to note that some desiccation-sensitive prokaryotes can possess resistance to IR (Beblo-Vranesevic et al. 2018).

In this context, the 'radiation adaptation hypothesis' stipulates that desiccation tolerance could be a consequence to IR, as gene products contributing to IR may have been recruited in some microbes to serve an additional function that is desiccation tolerance (Sghaier et al. 2007). The multi-resistance of isolate PT9^T may be originating from its oxidative response mechanisms. Thus, the genome sequencing of PT9^T was performed to identify these mechanisms and the strategies used to thrive under extreme conditions, such as gamma radiation, desiccation, salt concentration, H_2O_2 , etc.

Genome sequence analysis and oxidative stress response

Genomic features

The complete genome of *P. panici* PT9^T consists of 6,582,650 bps in size and has an average G+C content of 71.2%. The size of the PT9^T chromosome is not similar to this of the most closely related strain *P. soli* CGMCC 4.7398^T (5,378,526 bps). De novo assembly of the genome sequencing data of PT9^T resulted in 59 contigs and an average CDS length of 984.18 bp. The genome was predicted to contain 6368 protein-coding genes, with a 91.9% protein-coding density, 51 tRNA and 3 rRNA genes. General

501 features for the complete genome of PT9^T are shown in
502 Table 2.

503 For 6291 protein-coding genes, 75.08% (4723 CDSs)
504 are classified in at least one Clusters of Orthologous Genes
505 (COG) group. The most abundant categories are general
506 function prediction (910); carbohydrate transport and
507 metabolism (808); transcription (744); amino acid trans-
508 port and metabolism (610); and inorganic ion transport and
509 metabolism (405). The identification also of several categor-
510 ies involved in the defense of microorganisms, which are
511 cell wall/membrane/envelope biogenesis (270); replication,
512 recombination and repair (200); secondary metabolites bio-
513 synthesis, transport and catabolism (175); chaperones (151);
514 defense mechanisms (116); and more others (Supporting
515 information presented in Table S2).

516 Prediction of genes related to oxidative stress response

517 The genome sequence of PT9^T contains several genes impli-
518 cated in response to oxidative stress (Table 3).

519 Several proteins detected in isolate PT9^T were reported
520 to have a role in IR and desiccation resistance-associated
521 mechanisms such as GyrAB, NucS, PolA, RadA, RecA,
522 RecD, RecO, SodA, SoxR, SSB and UvrD (Lim et al. 2019).
523 PT9^T contains also various proteins implicated in defense
524 mechanisms related to oxidative stress response, such as uni-
525 versal stress protein UspA, class III stress response-related
526 ATPase ClpC, Fe-S center for redox-sensing, putative ATP-
527 dependent helicase DinG, putative ABC transporter YclH,
528 ferric enterobactin transport ATP-binding protein FepC,
529 daunorubicin/doxorubicin resistance ATP-binding protein
530 DrrA. The proteins observed in response to oxidative stress
531 of *D. radiodurans* were DNA repair proteins (PolA, RadA,
532 RecA, RecF, RecO), DNA protein binding (ArgF, DnaE,
533 HisS, RecN), ribosomal proteins (RplB, RpsI, RpsR) and
534 oxidation–reduction process proteins (GltA, NuoC) (Slade
535 et al. 2009; Ujaoney et al. 2017; Gao et al. 2020).

536 Isolate PT9^T seems to possess genes involved in the
537 protection of its cytosolic proteins from oxidation (such as
538 *mntA*, *mntB*, *sodA*) and the repair of DNA double-strand
539 breaks (DSBs) after exposure to IR (*dinG*, *hup*, *recA*, *recQ*,
540 *ssbA*) (Lim et al. 2019). Several DNA repair genes, which
541 were reported to contribute to radiation and oxidative stress
542 resistance in *D. radiodurans*, such as *gyrAB*, *ligD*, *ligA*, *recC*
543 (Bellenberg et al. 2019; Lim et al. 2019), were also detected
544 in the genome of isolate PT9^T. Some genes of *D. radio-*
545 *durans*, such as *recF* and *recO*, are extremely sensitive to
546 gamma rays, which are required for recombination repair
547 by an incomplete genome reconstitution, a reduced level of
548 DNA breakdown and an absence of DNA synthesis (Bent-
549 chikou et al. 2010). *RecF* and *RecO* genes play an essential
550 role in DNA double-strand-break repair pathways through
551 an extended synthesis-dependent strand annealing process

(ESDSA) (Bentchikou et al. 2010), which might be involved
552 in the repair of DSBs and the DNA synthesis step of ESDSA
553 for isolate PT9^T.
554

555 Furthermore, the treatment of *D. radiodurans* R1 with IR
556 (and also desiccation) induced the over-expression of several
557 genes in responses to oxidative stress damages, such as *recA*
558 and *uvrD*, which encode proteins that have been previously
559 associated with DNA repair (Tanaka et al. 2004).

560 PT9^T contains also many DNA ligase paralogs (such as
561 *ligA*, *ligC*, *ligD*) and putative DNA ligases. For instance,
562 *ligD* gene is involved in the bacterial non-homologous DNA
563 end joining (NHEJ) pathway according to the study of Ishino
564 and Narumi (2015). *D. radiodurans* possesses efficient oxi-
565 dative damage protection mechanisms, such as NHEJ and
566 CNDEJ (condensed nucleoid-dependent end joining) repair
567 pathways, involving radiation-inducible proteins (Ishino and
568 Narumi 2015). These DNA repair proteins, such as ATP-
569 dependent DNA ligase that was detected in the genome of
570 PT9^T, play a principal role in the CNDEJ pathway, which
571 represents a DSBs repair system specific to radioresistant
572 bacteria with a high degree of genome condensation.

573 PT9^T contains also desiccation tolerance-associated pro-
574 teins, such as ferritin BfrB, pleiotropic regulatory protein
575 DegT, HTH-type transcriptional regulator RcdA, manga-
576 nese-containing peroxidase XpdC (Mn_catalase) (Lim et al. 2019).
577

578 Various enzymes involved in oxidative stress responses,
579 such as catalase, superoxide dismutase, NADH-dependent
580 oxidases, manganese-containing antioxidants, which provide
581 an important role to protect radioresistant microorganisms
582 (Cárdenas et al. 2012; Bellenberg et al. 2019). Catalase
583 KatA, superoxide dismutase [Mn] SodA and manganese
584 MntA were detected in the genome of PT9^T.

585 Radioresistant microorganisms have various mecha-
586 nisms of defense against ionizing radiation, desiccation,
587 oxidative stress-generating agents and environmental
588 stresses that can damage cell components, including the
589 production of scavenging ROS, detoxification and repair
590 systems (Lim et al. 2019). *Deinococcus radiodurans*, has
591 developed efficient enzymatic and non-enzymatic anti-
592 oxidant systems, involving different physiological deter-
593 minants and well-regulated molecular mechanisms for
594 tolerance to radiation, desiccation and oxidative stress
595 (Timmins and Moe 2016; Bellenberg et al. 2019). *D. radi-*
596 *odurans* employs various strategies to prevent oxidative
597 stress, including an efficient DNA repair system, ROS-
598 scavenging enzymes (catalase and superoxide dismutase),
599 non-enzymatic antioxidants and transcriptional regulators
600 (OxyR) (Munteanu et al. 2015; Chen et al. 2019). The
601 genome sequence of *D. radiodurans* revealed the pres-
602 ence of homologues of most well-known prokaryotic DNA
603 repair proteins involved in base excision repair, nucleotide
604 excision repair, mismatch repair and recombination repair.

Table 3 List of genes involved in response to oxidative stress

Label	Length (pb)	Gene	Functional
PROM_v1_370013	1239	<i>recF</i>	DNA replication and repair protein RecF
PROM_v1_20039	1449	<i>kata</i>	Scavenge (Catabolism) vegetative catalase 1
PROM_v1_40259	2232	<i>katG</i>	Catalase/hydroperoxidase HPI(I)
PROM_v1_70135	606	<i>recR</i>	RecA filament-DNA complex stabilisation factor
PROM_v1_470015	510	<i>dps</i>	DNA protection during starvation protein
PROM_v1_210103	1848	<i>recQ</i>	ATP-dependent DNA helicase RecQ
PROM_v1_10004	549	<i>ssbA</i>	Single-strand DNA-binding protein SSB
PROM_v1_10142	2628	<i>clpB</i>	Protein disaggregation chaperone
PROM_v1_50101	963	<i>drrA</i>	Daunorubicin/doxorubicin resistance ATP-binding protein DrrA
PROM_v1_330032	1779	–	UMUC domain protein DNA-repair protein
PROM_v1_270047	3621	<i>mfd</i>	Transcription-repair-coupling factor
PROM_v1_230011	1755	<i>recN</i>	DNA repair protein RecN
PROM_v1_20182	1224	<i>recA</i>	Multifunctional SOS repair factor
PROM_v1_40053	747	<i>recO</i>	DNA repair protein RecO
PROM_v1_40152	2496	<i>ligD</i>	Multifunctional non-homologous end joining DNA repair protein LigD
PROM_v1_240013	2412	<i>ligA</i>	DNA ligase
PROM_v1_10007	237	–	Ribosomal protein S18 RpsR
PROM_v1_170101	375	–	Ribosomal protein S12 (BS12) RpsL
PROM_v1_170093	837	–	Ribosomal protein L2 (BL2) RplB
PROM_v1_90068	1578	<i>lig</i>	Putative DNA ligase
PROM_v1_120124	1182	<i>ligC</i>	DNA ligase C
PROM_v1_40293	1518	<i>obgE</i>	ppGpp-binding GTPase involved in cell portioning; DNA repair and ribosome assembly
PROM_v1_90030	465	<i>atl1</i>	Alkylated DNA nucleotide flippase At1; Ada-like DNA-binding domain: nucleotide excision repair
PROM_v1_140011	1119	–	DNA alkylation repair protein
PROM_v1_190139	1443	<i>radA</i>	DNA repair protein
PROM_v1_20165	2106	<i>dinG</i>	putative ATP-dependent helicase DinG homolog
PROM_v1_220099	447	<i>rnhA</i>	DNA replication, recombination, and repair; Degradation of proteins, peptides, and glycopeptides
PROM_v1_10046	456	–	Nucleotide-binding universal stress protein: UspA family
PROM_v1_140049	510	–	Universal stress protein UspA
PROM_v1_190003	2562	<i>clpC mecB</i>	Class III stress response-related ATPase, AAA + superfamily
PROM_v1_200143	489	<i>soxR marC</i>	DNA-binding transcriptional dual regulator, Fe-S center for redox-sensing
PROM_v1_28004	837	–	Ser/Thr protein kinase RdoA involved in Cpx stress response
PROM_v1_350012	396	–	Universal stress protein MSMEG_4207
PROM_v1_380020	420	–	Stress response protein
PROM_v1_480007	660	–	Putative stress-induced transcription regulator
PROM_v1_20114	204	<i>cspD</i>	Cold-shock protein, molecular chaperone, RNA-helicase co-factor
PROM_v1_50089	2478	<i>gyrA</i>	DNA gyrase subunit A
PROM_v1_250073	2211	<i>gyrB</i>	DNA gyrase subunit B
PROM_v1_10073	282	<i>hup</i>	DNA-binding protein HB1
PROM_v1_120020	2637	<i>polA</i>	DNA polymerase I
PROM_v1_50212	3378	<i>recB</i>	RecBCD enzyme subunit RecB
PROM_v1_50213	3402	<i>recC</i>	RecBCD enzyme subunit RecC
PROM_v1_50211	1866	<i>recD</i>	RecBCD enzyme subunit RecD
PROM_v1_30191	2067	<i>uvrD</i>	ATP-dependent DNA helicase UvrD2
PROM_v1_20292	810	<i>feuV</i>	Iron(III)-siderophore transporter: ATP binding component
PROM_v1_50182	882	<i>xpdC</i>	Phage PBSX; manganese-containing peroxidase
PROM_v1_150073	873	<i>mntA</i>	Manganese transport system ATP-binding protein MntA
PROM_v1_150072	864	<i>mntB</i>	Manganese transport system ATP-binding protein MntB

Table 3 (continued)

Label	Length (pb)	Gene	Functional
PROM_v1_290076	894	<i>mntC</i>	Manganese transport system ATP-binding protein MntC
PROM_v1_20214	1230	–	Mn ²⁺ and Fe ²⁺ transporters of the NRAMP family
PROM_v1_230090	1308	<i>mntH</i>	Divalent metal cation transporter MntH
PROM_v1_250040	630	<i>sodA</i>	Superoxide dismutase [Mn]
PROM_v1_70011	753	–	Fe(3+)-transporting ATPase
PROM_v1_180005	1566	<i>fbpB</i>	Fe(3+)-transport system permease protein SfuB
PROM_v1_150099	789	<i>fepC</i>	Ferric enterobactin transport ATP-binding protein FepC
PROM_v1_80082	1320	–	Mn ²⁺ and Fe ²⁺ transporters of the NRAMP family
PROM_v1_20146	825	<i>fecE</i>	Iron-dicitrate transporter subunit
PROM_v1_20290	1020	<i>fecD</i>	Iron-dicitrate ABC transporter (permease)
PROM_v1_240047	1308	<i>gltA</i>	Glutamate synthase (large subunit, NADP-dependent)
PROM_v1_80125	762	<i>nuoC</i>	NADH-quinone oxidoreductase subunit C
PROM_v1_120112	1380	<i>hisS</i>	Histidine-tRNA ligase
PROM_v1_20071	3552	<i>dnaE</i>	DNA polymerase III subunit alpha
PROM_v1_20016	948	<i>argF</i> <i>argC</i>	Ornithine carbamoyltransferase
PROM_v1_400015	696	<i>nucS</i>	Endonuclease NucS

605 Thus, the DNA repair machinery of *D. radiodurans* seems
606 similar to that of other bacteria, such as isolate PT9^T, with
607 specificities contributing to radiation resistance and pro-
608 tection of proteins against oxidative damages (Makarova
609 et al. 2001; Daly 2012; Lim et al. 2019).

610 To conclude, oxidative stress resistance of PT9^T against
611 damages caused by gamma radiation, desiccation and
612 oxidative stress generated by H₂O₂ was explained by the
613 presence of a combination of enzymatic anti-oxidants
614 (ROS-scavenging enzymes, such as catalase, superox-
615 ide dismutase) and non-enzymatic (like carotenoids and
616 manganese Mn²⁺) defense mechanisms (Shashidhar et al.
617 2010; Slade and Radman 2011). These proteins are mainly
618 associated with DNA repair and response to oxidative
619 stress. Further functional analyses of these new oxidative
620 stress-induced proteins will enhance our understanding of
621 the regulatory mechanism underlying extreme resistance
622 to oxidative stress in isolate PT9^T. However, sufficient pro-
623 teome protection is crucial for survival after irradiation
624 because protein activity is required for essential processes

including transcription, translation and DNA repair (Bel-
lenberg et al. 2019).

Secondary metabolites prediction

627
628 The genome analysis of isolate PT9^T harbors multiple
629 secondary metabolites related to defense mechanisms and
630 strategies developed to survive under extreme conditions
631 (Table 4).

632 As shown in Table 4, five biosynthesis gene clusters for
633 secondary metabolites were identified in the genome of iso-
634 late PT9^T—oligosaccharides, t3pks, lassopeptides, sidero-
635 phores and ectoine.

636 Various microbial metabolites, such as oligosaccha-
637 rides, carotenoids and compatible solutes (ectoine) were
638 demonstrated to protect cells against IR (Beblo-Vranesevic
639 et al. 2017). Cupriabactin is a carboxylate-type siderophore
640 extracted from *Cupriavidus necator* JMP134, which demon-
641 strated important roles in iron scavenging, bacterial motility,
642 biofilm formation and oxidative stress resistance. Physiolog-
643 ical analyses revealed that this system induced an increase

Table 4 AntiSMASH secondary metabolites of *P. panici* PT9^T

Cluster	Cluster type	Most similar known cluster	Length (bp)
1	Oligosaccharide	Oligosaccharide	51,475
2	t3pks	Arylomycin biosynthesis Alkylresorcinol, Clarexopoxcin, Polyketide	41,116
3	Lassopeptide	SapB biosynthesis	22,426
4	Siderophore	Desferrioxamine B biosynthesis	12,643
5	Ectoine	Ectoine biosynthesis	8697

of the resistance of *C. necator* JMP134 to stress caused by aromatic compounds (Li et al. 2019). In general, oxidative stress responses of bacteria have been observed to be part of complex phenomena such as biofilm formation, antibiotic resistance and pathogenicity (Cárdenas et al. 2012). Also, a secondary defense barrier consists of the induced expression of specific ROS degrading enzymes and repair systems for damaged macromolecules (Cabiscol et al. 2000).

Altogether, our findings allow us to develop an integrated understanding of the molecular basis of recovery from desiccation and other protein and DNA-damaging agents in PT9^T and roots-associated bacteria, particularly in the extreme environment of the Tunisian desert.

Description of *Promicromonospora panici* sp. nov.

Promicromonospora panici [pa'ni.ci. N.L. gen. n. *panici* referring to the isolation source, the xerophytic plant *Panicum*].

Aerobic, Gram-staining positive, non-spore-forming and non-motile actinobacterium. Forms well-developed branching septate hyphae that breaks up into fragments of various sizes and rod-shaped elements on the media tested after incubation at 30 °C for 72 h. Colonies are white to yellowish-white with characteristic wrinkly surfaces. Cells grow well on soya flour mannitol, nutrient agar and tryptic soy agar media, but no growth was observed on LB agar medium. Optimal growth occurs at 28–37 °C (optimum at 30 °C) and pH 6.0–9.0. No growth in the presence of 2% NaCl. Positive for catalase and oxidase.

The major fatty acids are anteiso-C15:0 and iso-C15:0. The polar lipid pattern is diphosphatidylglycerol (DPG), phosphatidylglycerol (PG), phosphatidylinositol (PI), phosphoglycolipid (PGL), unidentified glycolipids (GL₁₋₃), lipid (L) and phospholipid (PL). Whole-organism hydrolysates contain DL-2,6-diaminopimelic acid (DL-DAP), galactose, glucose and ribose as whole cell sugars.

The genome of the type strain is 6.5 Mb with a GC content of 71.2 mol%. The GenBank/ENA accession number for the draft genome sequence of isolate PT9^T is PRJEB29453.

The type strain PT9^T (LMG 31103^T = DSM 108613^T) was isolated from irradiated roots of *P. turgidum* collected from the Ksar Ghilane oasis, southern Tunisia.

Acknowledgement This work was performed under the auspices of Université Lyon 1, CNRS UMR 5557, Écologie Microbienne (France) and the National Center for Nuclear Sciences and Technology CNSTN (Tunisia) and in the ambit of the BIODESERT research program of the LR11-ES31 (BVBGR, ISBST, University of Manouba). The LAB-GeM (CEA/Genoscope & CNRS UMR8030), the France Génomique and French Bioinformatics Institute national infrastructures (funded as part of Investissement d'Avenir program managed by Agence Nationale pour la Recherche, contracts ANR-10-INBS-09 and ANR-11-INBS-0013) are acknowledged for support within the MicroScope annotation platform. We thank Betty Bigai, Corinne Sannaire and

platform Genomique Environmental PGE, UMR CNRS 5557 for technical support.

Compliance with ethical standards

Conflict of interest The authors declare no conflict of interest.

References

- Basu B, Apte SK (2012) Gamma radiation-induced proteome of *Deinococcus radiodurans* primarily targets DNA repair and oxidative stress alleviation. *Mol Cell Proteom* 11(M111):011734
- Beblo-Vranesevic K, Galinski EA, Rachel R, Huber H, Rettberg P (2017) Influence of osmotic stress on desiccation and irradiation tolerance of (hyper)-thermophilic microorganisms. *Arch Microbiol* 199:17–28
- Beblo-Vranesevic K, Bohmeier M, Perras AK et al (2018) Lack of correlation of desiccation and radiation tolerance in microorganisms from diverse extreme environments tested under anoxic conditions. *FEMS Microbiol Lett* 365(6):fny044
- Bellenberg S, Huynh D, Poetsch A, Sand W, Vera M (2019) Proteomics reveal enhanced oxidative stress responses and metabolic adaptation in *Acidithiobacillus ferrooxidans* biofilm cells on pyrite. *Front Microbiol* 10:592
- Benhamda C, Benkahla A, Ben Miled S, Ouled-Haddar H, del Carmen MC, Gtari M, Cherif A, Hofner B, Gjedira K, Sghaier H (2015) The RadioP1—an integrative web resource for radioresistant prokaryotes. *Intech Open*, London, pp 89–105
- Bentchikou E, Servant P, Coste G, Sommer S (2010) A major role of the RecFOR pathway in DNA double-strand-break repair through ESDSA in *Deinococcus radiodurans*. *PLoS Genet* 6:e1000774
- Blin K, Medema MH, Kazempour D, Fischbach MA, Breitling TRE, Weber T (2013) AntiSMASH 2.0—a versatile platform for genome mining of secondary metabolite producers. *Nucleic Acids Res* 41:W204–W212
- Busse HJ, Zlamala C, Buczolits S, Lubitz W, Kämpfer P, Takeuchi M (2003) *Promicromonospora vindobonensis* sp. nov. and *Promicromonospora aerolata* sp. nov., isolated from the air in the medieval 'Virgilkapelle' in Vienna. *Int J Syst Evol Microbiol* 53:1503–1507
- Cabiscol E, Tamarit J, Ros J (2000) Oxidative stress in bacteria and protein damage by reactive oxygen species. *Internal Microbiol* 3:3–8
- Cárdenas JP, Moya F, Covarrubias P, Shmaryahu A, Levicán G, Holmes DS et al (2012) Comparative genomics of the oxidative stress response in bioleaching microorganisms. *Hydrometallurgy* 12:162–167
- Castro-Wallace SL, Chiu CY, John KK, Stahl SE, Rubins KH et al (2017) Nanopore DNA sequencing and genome assembly on the international space station. *Sci Rep* 7:18022
- Chen Y, Xue D, Sun W, Han J, Li J, Gao R, Zhou Z, Zhang W, Chen M, Lin M et al (2019) SRNA OsiA stabilizes catalase mRNA during oxidative stress response of *Deinococcus radiodurans* R1. *Microorganisms* 7:e422
- Chun J, Oren A, Ventosa A, Christensen H, Arahal DR, da Costa MS, Rooney AP, Yi H, Xu XW, De Meyer S, Trujillo ME (2018) Proposed minimal standards for the use of genome data for the taxonomy of prokaryotes. *Int J Syst Evol Microbiol* 68:461–466
- Daly MJ (2012) Death by protein damage in irradiated cells. *DNA Repair (Amst)* 11:12–21
- Flandrois JP, Perriere G, Gouy M (2015) leBIBIQBPP: a set of databases and a web tool for automatic phylogenetic analysis of prokaryotic sequences. *BMC Bioinform* 16:251

- 755 Gabani P, Singh OV (2013) Radiation-resistant extremophiles and their
756 potential in biotechnology and therapeutics. *Appl Microbiol Bio-*
757 *technol* 97:993–1004
- 758 Gao L, Zhou Z, Chen X, Zhang W, Lin M, Chen M (2020) Comparative
759 proteomics analysis reveals new features of the oxidative stress
760 response in the polyextremophilic bacterium *Deinococcus radio-*
761 *durans*. *MDPI J Microorgan* 8:451
- 762 Gholami M, Etemadifar Z, Bouzari M (2015) Isolation a new strain of
763 *Kocuria rosea* capable of tolerating extreme conditions. *J Environ*
764 *Radioact* 144:113–119
- 765 Goris J, Konstantinidis KT, Klappenbach JA, Coenye T, Vandamme
766 P, Tiedje JM (2007) DNA-DNA hybridization values and their
767 relationship to whole-genome sequence similarities. *Int J Syst*
768 *Evol Microbiol* 57(1):81–91
- 769 Guindon S, Dufayard JF, Lefort V, Anisimova M, Hordijk W, Gascuel
770 O (2010) New algorithms and methods to estimate maximum-
771 likelihood phylogenies: assessing the performance of PhyML 3.0.
772 *System Biol* 59(3):307–321
- 773 Guo L, Liu C, Zhao J, Li C, Guo S, Fan J, Li J, Wang X, Xiang W
774 (2016) *Promicromonospora alba* sp. nov., an actinomycete iso-
775 lated from the cuticle of *Camponotus japonicas* Mayr. *Int J Syst*
776 *Evol Microbiol* 66:1340–1345
- 777 Hamed J, Dehghani M, Mohammdipناه F (2015) Isolation of
778 extremely heavy metal resistant strains of rare actinomycetes from
779 high metal content soils in Iran. *Int J Environ Res* 9(2):475–480
- 780 Izumikawa M, Takagi M, Shin-Ya K (2011) Isolation of a novel mac-
781 rocyclic dilactone-JBIR-101-from *Promicromonospora* sp. RL26.
782 *J Antibiot* 64:689–691
- 783 Jin L, Zhao J, Jiang S, Zhao Y, Han X, Guo X, Wang X, Xiang W
784 (2018) *Promicromonospora viridis* sp. nov., a novel actinomycete
785 isolated from soil. *Antonie van Leeuwenhoek*
- 786 Kaewkla O, Franco CMM (2017) *Promicromonospora callitridis* sp.
787 nov., an endophytic actinobacterium isolated from the surface-
788 sterilized root of an Australian native pine tree. *Int J Syst Evol*
789 *Microbiol* 67:3559–3563
- 790 Kaewkla O, Franco CMM (2019) *Actinomycetospora callitridis* sp.
791 nov., an endophytic actinobacterium isolated from the surface-
792 sterilized root of an Australian native pine tree. *Antonie Van Leeu-*
793 *wenhoek* 112:331–337
- 794 Kang SM, Khan AL, Hamayun M, Hussain J, Joo GJ, You YH, Kim
795 JG, Lee IJ (2012) Gibberellin-producing *Promicromonospora* sp.
796 SE188 improves *Solanum lycopersicum* plant growth and influ-
797 ences endogenous plant hormones. *J Microbiol* 50:902–909
- 798 Kang SM, Khan AL, Waqas M, You YH, Kim JH, Kim JG, Hamayun
799 M, Lee IJ (2014) Plant growth promoting rhizobacteria reduce
800 adverse effects of salinity and osmotic stress by regulating phy-
801tohormones and antioxidants in *Cucumis sativus*. *J Plant Interact*
802 9:673–682
- 803 Krasilnikov NA, Kalakoutskii LV, Kirillova NF (1961) A new genus of
804 Actinomycetales, *Promicromonospora* gen. nov. vol 1. *Bull Acad*
805 *Sci USSR (Ser Biol)*.
- 806 Kroppenstedt RM, Goodfellow M (2006) The family Thermomonos-
807 sporaceae: Actinocorallia, Actinomadura, Spirillisporea and Ther-
808 momonospora. *Archaea, Bacteria, Firmicutes, Actinomycetes*. In:
809 Dworkin M, Falkow S, Rosenberg E, Schleifer KH, Stackebrandt
810 E (eds) *The prokaryotes: a handbook the biology of bacteria*.
811 Springer, New York, pp 682–724
- 812 Kumar M, Joshi A, Kashyap R, Khanna S (2011) Production of xyla-
813 nase by *Promicromonospora* sp. MARS with rice straw under non
814 sterile conditions. *Process Biochem* 46:1614–1618
- 815 Lechevalier MP, Lechevalier HA (1970) Chemical composition as a
816 criterion in the classification of aerobic actinomycetes. *Int J Syst*
817 *Bacteriol* 20:435–443
- 818 Li WJ, Xu P, Schumann P, Zhang YQ, Pukall R, Xu LH, Stack-
819 ebrandt E, Jiang CL (2007) *Georgenia ruanii* sp. nov., a novel
820 actinobacterium isolated from forest soil in Yunnan (China),
and emended description of the genus *Georgenia*. *Int J Syst*
821 *Evol Microbiol* 57:1424–1428
- 822 Li C, Zhu L, Pan D, Li S, Xiao H, Zhang Z, Shen X, Wang Y, Long M
823 (2019) Siderophore mediated iron acquisition enhances resist-
824 ance to oxidative and aromatic compound stress in *Cupriavidus*
825 *neccator* JMP134. *Appl Environ Microbiol* 85:e01938–e2018
- 826 Lim S, Jung JH, Blanchard L, de Groot A (2019) Conservation and
827 diversity of radiation and oxidative stress resistance mechanisms
828 in *Deinococcus* species. *FEMS Microbiol Rev* 43(1):19–52
- 829 Makarova KS, Aravind L, Wolf YI, Tatusov RL, Minton KW,
830 Koonin EV, Daly MJ (2001) Genome of the extremely radiation-
831 resistant bacterium *Deinococcus radiodurans* viewed from the
832 perspective of comparative genomics. *Microbiol Mol Biol R*
833 *ev* 65:44–79
- 834 Marmur J (1961) A procedure for the isolation of deoxyribonucleic
835 acid from microorganisms. *J Mol Biol* 3:208
- 836 Mattimore Battista VJR (1996) Radioresistance of *Deinococcus*
837 *radiodurans*: functions necessary to survive ionizing radiation
838 are also necessary to survive prolonged desiccation. *J Bacteriol*
839 178:633–637
- 840 Medema MH, Blin K, Cimermancic P, de Jager V, Zakrzewski P, Fis-
841 chbach MA, Weber T, Takano E, Breitling R (2011) antiSMASH:
842 rapid identification, annotation and analysis of secondary metabo-
843 lite biosynthesis gene clusters in bacterial and fungal genome
844 sequences. *Nucleic Acids Res* 39:W339–W346
- 845 Meier-Kolthoff J, Göker M (2019) TYGS is an automated high-
846 throughput platform for state-of-the-art genome-based taxonomy.
847 *Nat Commun* 10:2182
- 848 Meier-Kolthoff JP, Auch AF, Klenk H-P, Göker M (2013) Genome
849 sequence-based species delimitation with confidence intervals and
850 improved distance functions. *BMC Bioinform* 14:60
- 851 Minh BQ, Nguyen AT, von Haeseler A (2013) Ultrafast approxima-
852 tion for phylogenetic bootstrap. *Mol Biol Evol* 30(5):1188–1195
- 853 Minnikin D, O'Donnell A, Goodfellow M, Alderson G, Athalye M,
854 Schaal A, Parlett JH (1984) An integrated procedure for the
855 extraction of bacterial isoprenoid quinones and polar lipids. *J*
856 *Microbiol Methods* 2:233–241
- 857 Mohammadipناه F, Montero-Calasanz MD, Schumann P, Sproer C,
858 Rohde M, Klenk HP (2017) *Promicromonospora kermanensis*
859 sp. nov., an actinobacterium isolated from soil. *Int J Syst Evol*
860 *Microbiol* 67:262–267
- 861 Morini J, Babini G, Barbieri S, Baiocco G, Ottolenghi A (2017) The
862 interplay between radioresistant Caco-2 cells and the immune sys-
863 tem increases epithelial layer permeability and alters signalling
864 protein spectrum. *Front Immunol* 8:233
- 865 Mosmann T (1983) Rapid colorimetric assay for cellular growth and
866 survival: application to proliferation and cytotoxicity assays. *J*
867 *Immunol Methods* 65:55–63
- 868 Munteanu A, Uivarosi V, Andries A (2015) Recent progress in under-
869 standing the molecular mechanisms of radioresistance in *Deino-*
870 *coccus* bacteria. *Extremophiles* 19:707–719
- 871 Qin S, Jiang JH, Klenk HP, Zhu WY, Zhao GZ, Zhao LX, Tang SK, Xu
872 LH, Li WJ (2012) *Promicromonospora xylanilytica* sp. nov., an
873 endophytic actinomycete isolated from surface-sterilized leaves of
874 the medicinal plant *Maytenus austroyunnanensis*. *Int J Syst Evol*
875 *Microbiol* 62:84–89
- 876 Richter M, Rossello-Mora R (2009) Shifting the genomic gold standard
877 for the prokaryotic species definition. *Proc Natl Acad Sci USA*
878 106:19126–19131
- 879 Schleifer KH, Kandler O (1972) Peptidoglycan types of bacterial cell
880 walls and their taxonomic implications. *Bacteriol Rev* 36:407–477
- 881 Schumann P, Stackebrandt E (2012) The family *Promicromono-*
882 *sporaceae*. Bergey's manual of systematic bacteriology. Springer,
883 New York
- 884 Schumann P, Weiss N, Stackebrandt E (2001) Reclassification of
885 *Cellulomonas cellulans* (Stackebrandt and Keddie 1986) as

- 887 *Cellulosimicrobium cellulans* gen. nov., comb. nov. Int J Syst Evol
888 Microbiol 51:1007–1010
- 889 Sghaier H, Narumi I, Satoh K, Ohba H, Mitomo H (2007) Problems
890 with the current deinococcal hypothesis: an alternative theory.
891 Theory Biosciences 126:43–45
- 892 Sghaier H, Ghedira K, Benkahla A, Barkallah I (2008) Basal DNA
893 repair machinery is subject to positive selection in ionizing-radi-
894 ation-resistant bacteria. BMC Genom 9:297
- 895 Shashidhar R, Kumar SA, Misra HS, Bandekar JR (2010) Evaluation
896 of the role of enzymatic and non-enzymatic antioxidant systems
897 in the radiation resistance of *Deinococcus*. Can J Microbiol
898 56:195–201
- 899 Slade D, Radman M (2011) Oxidative stress resistance in *Deinococcus*
900 *radiodurans*. Microbiol Mol Biol R 75:133–191
- 901 Slade D, Lindner AB, Paul G, Radman M (2009) Recombination and
902 replication in DNA repair of heavily irradiated *Deinococcus radi-*
903 *odurans*. Cell 136:1044–1055
- 904 Smibert R, Krieg N (1994) Phenotypic characterization. In: Gerhardt
905 P (ed) Methods for general and molecular bacteriology. American
906 Society for Microbiology, Washington, pp 607–654
- 907 Stackebrandt E, Ebers J (2006) Taxonomic parameters revisited: tar-
908 nished gold standards. Microbiol Today 33:152–155
- 909 Staneck JL, Roberts GD (1974) Simplified approach to identification
910 of aerobic actinomycetes by thin layer chromatography. J Appl
911 Microbiol 28:226–231
- 912 Sun LN, Zhang YF, He L, Chen ZJ, Wang QY, Qian M, Sheng XF
913 (2010) Genetic diversity and characterization of heavy metal-
914 resistant-endophytic bacteria from two copper-tolerant plant spe-
915 cies on copper mine wasteland. Bioresour Technol 101:501–509
- 916 Tanaka M, Earl AM, Howell HA, Park MJ, Eisen JA, Peterson SN,
917 Battista JR (2004) Analysis of *Deinococcus radiodurans*'s tran-
918 scriptional response to ionizing radiation and desiccation reveals
919 novel proteins that contribute to extreme radioresistance. Genet
920 Soc Am 168:21–33
- 921 Thomas L, Ram H, Kumar A, Singh VP (2016) Production, optimiza-
922 tion, and characterization of organic solvent tolerant cellulases
923 from a lignocellulosic waste-degrading actinobacterium, *Promi-*
924 *cromonospora* sp. VP111. Appl Biochem Biotechnol 179:863–879
- 925 Timmins J, Moe E (2016) A decade of biochemical and structural stud-
926 ies of the DNA repair machinery of *Deinococcus radiodurans*:
927 major findings, functional and mechanistic insight and challenges.
928 Comput Struct Biotechnol J 14:168–176
- Trifinopoulos J, Nguyen LT, von Haeseler A, Minh BQ (2016) W-IQ-
TREE: a fast online phylogenetic tool for maximum likelihood
analysis. Nucleic Acids Res 44:232–235
- Ujaoney AK, Padwal MK, Basu B (2017) Proteome dynamics during
post-desiccation recovery reveal convergence of desiccation and
gamma radiation stress response pathways in *Deinococcus radi-*
odurans. Biochim Biophys Acta Proteins Proteom 1865:1215–1226
- Vallenet D, Calteau A, Cruveiller S, Gachet M, Lajus A, Josso A, Mer-
cier J, Renaux A, Rollin J, Rouy Z, Roche D, Scarpelli C, Médigue
C (2017) MicroScope in 2017: an expanding and evolving inte-
grated resource for community expertise of microbial genomes.
Nucleic Acids Res 45:517–528
- Ventorino V, Aliberti A, Faraco V, Robertiello A, Giacobbe S, Ercolini
D, Amore A, Fagnano M, Pepe O (2015) Exploring the microbiota
dynamics related to vegetable biomasses degradation and study of
lignocellulose-degrading bacteria for industrial biotechnological
application. Sci Rep 5:8161
- Wayne LG, Brenner DJ, Colwell RR, Grimont PAD, Kandler O,
Krichevsky MI, Moore LH, Moore WEC, Murray RGE, Stack-
ebrandt E, Starr MP, Truper HG (1987) Report of the Ad Hoc
Committee On Reconciliation Of Approaches To Bacterial Sys-
tematics. Int J Syst Evol Microbiol 37:463–464
- Weber T, Blin K, Duddela S et al (2015) antiSMASH 3.0—a comprehen-
sive resource for the genome mining of biosynthetic gene clusters.
Nucleic Acids Res 43:237–243
- Yoon SH, Ha SM, Kwon S, Lim J, Kim Y, Seo H, Chun J (2017)
Introducing EzBioCloud: a taxonomically united database of 16S
rRNA gene sequences and whole-genome assemblies. Int J Syst
Evol Microbiol 67:1613–1617
- Zheng W, Li D, Zhao J, Liu C, Zhao Y, Xiang W, Wang X (2017)
Promicromonospora soli sp. nov., a novel actinomycete isolated
from soil. Int J Syst Evol Microbiol 67:3829–3833
- Zothanpuia PAK, Leo VV, Chandra P, Kumar B, Nayak C, Hashem A,
Abd-Allah EF, Alqarawi AA, Singh BP (2018) Bioprospection of
actinobacteria derived from freshwater sediments for their poten-
tial to produce antimicrobial compounds. Microb Cell Fact 17:68
- Publisher's Note** Springer Nature remains neutral with regard to
jurisdictional claims in published maps and institutional affiliations.

Affiliations

Sihem Guesmi^{1,2} · Imen Nouioui^{3,4} · Petar Pujic^{5,6} · Audrey Dubost^{5,6} · Afef Najjari⁷ · Kais Ghedira⁸ · José M. Igual⁹ ·
Ameur Cherif¹⁰ · Hans-peter Klenk³ · Haïtham Sghaier^{2,10} · Philippe Normand^{5,6}

¹ National Agronomy Institute of Tunisia, Avenue Charles Nicolle, 1082 Tunis, Mahrajène, Tunisia

² Laboratory “Energy and Matter for Development of Nuclear Sciences” (LR16CNSTN02), National Center for Nuclear Sciences and Technology, Sidi Thabet Technopark, 2020 Sidi Thabet, Tunisia

³ School of Natural and Environmental Sciences, Newcastle University, Ridley Building 2, Newcastle upon Tyne NE1 7RU, UK

⁴ Leibniz Institute DSMZ-German Collection of Microorganisms and Cell Cultures, Braunschweig, Germany

⁵ Université de Lyon, Université Lyon 1, Lyon, France

⁶ CNRS, UMR 5557, Écologie Microbienne, UMR1418, INRA, 69622 Villeurbanne Cedex, France

⁷ Université de Tunis el Manar, Faculté des Sciences de Tunis, LR03ES03 Microorganismes et Biomolécules Actives, 2092 Tunis, Tunisia

⁸ Laboratory of Bioinformatics, Biomathematics and Biostatistics-LR16IPT09, Institut Pasteur de Tunis, Université de Tunis El Manar, 1002 Tunis, Tunisia

⁹ Instituto de Recursos Naturales y Agrobiología de Salamanca, Consejo Superior de Investigaciones Científicas (IRNASA-CSIC), c/Cordel de Merinas 40-52, 37008 Salamanca, Spain

¹⁰ University Manouba, ISBST, BVBGR-LR11ES31.,
Biotechpole Sidi Thabet, 2020 Ariana, Tunisia

UNCORRECTED PROOF